

Real-Time Implementation of L1 RTK System Based on Position-Domain Hatch filter

Hee-Sung Kim

School of Electronics, Telecommunication & Computer, Korea Aerospace University,
Korea, hskim07@kau.ac.kr

Hyung Keun Lee

School of Electronics, Telecommunication & Computer, Korea Aerospace University,
Korea, hyknlee@kau.ac.kr

ABSTRACT

Real Time Kinematic (RTK) positioning techniques have been useful for various application areas which require precise position information. To enlarge the possible application area of the RTK techniques furthermore, it is necessary to enable the RTK positioning by low-cost L1-only single-frequency GNSS receivers. In this study, an L1 RTK system based on the position domain Hatch filter is designed and implemented. For the utilization of low-cost single-frequency receivers in L1 RTK positioning, a compensation method for clock offset and clock jump is proposed. The performance of the proposed L1 RTK system is demonstrated by a 4.9 km-baseline real-data experiment.

INTRODUCTION

The Real Time Kinematic (RTK) technique is

one the most popular methods to acquire precise cm-level position information in real-time. Compared with the conventional DGPS/DGNSS techniques utilizing both the code and the carrier phase measurements, the RTK techniques are based only on the carrier phase measurements since the noise magnitude of carrier phase measurements is much smaller than that of code measurement. To obtain accurate position estimate based on the carrier phase measurements, unknown integer ambiguities should be resolved. Thus, it is important to achieve reliable and fast ambiguity resolution. By investigating the previous research works on the RTK techniques, it can be seen they are usually based on high-quality dual-frequency receivers, consider slowly-moving or static receivers for real-time implementation. It can also be seen that both the reference and mobile receivers are of the same hardware type from the same manufacturer.

The application area of the RTK techniques is

required to be enlarged furthermore considering unimaginable future potentials. To enlarge the possible application area of the RTK techniques, it is necessary to enable the RTK positioning by low-cost single-frequency GNSS receivers. However, the implementation of the L1 RTK system by low-cost highly-dynamic receivers is not easy since wide-lane carrier phase combinations cannot be utilized as in the case of dual-frequency RTK systems.

In this study, an L1 RTK system based on the position domain Hatch is designed and implemented.

To provide sufficiently good environment for L1-only integer ambiguity resolution, the double-differencing (DD) position-domain (PD) Hatch filter [3] is utilized. The DD PD Hatch filter forms accurate and reliable float solutions with consistent error covariance information under frequent changes in visible satellites. To utilize low-cost single-frequency receivers as L1 RTK platforms, a compensation method for clock offset and clock jump is proposed. To verify the performance of the proposed L1 RTK system, a 4.9 km static baseline experiment was performed and analyzed.

DOUBLE DIFFERENCING POSITION DOMAIN HATCH FILTER

The range domain (RD) carrier-smoothed-code filtering proposed by Hatch [1] is a good example of an algorithm that maximally utilizes the information redundancy provided by GNSS to improve positioning accuracy. Based on the conventional RD Hatch filtering, the single differencing (SD) PD Hatch filter was proposed

in [2] to generate consistent and realistic error covariance information under frequent changes in visible satellites.

It was also shown that the SD PD Hatch filter generates white residual sequence like the conventional RD Hatch filter for short-baseline applications. Recently, to eliminate the effects of the clock bias dynamics and to consider the extension for networked RTK applications, the DD PD Hatch filter was proposed in [5]. The DD PD Hatch filter is summarized in Table 1.

Table 1. DD PD Hatch filter

Initialization
$\mathbf{H}_{k0}^* = \Gamma_{k0} \mathbf{H}_{k0}$ $\hat{\mathbf{X}}_{k0} = E[X_{k0} \Gamma_{k0} \tilde{\rho}_{k0}^{jo}], \hat{\mathbf{P}}_{k0} = [(\mathbf{H}_{k0})^T (R_{\rho,k0})^{-1} \mathbf{H}_{k0}]^T$
Time-Propagation
$\mathbf{H}_k^* = \Gamma_k \mathbf{H}_k, \mathbf{H}_k^p = \Gamma_k \mathbf{H}_k, \Omega_k^* = \Gamma_k \Omega_k$ $\mathbf{R}_{\phi,k}^* = \Gamma_k \mathbf{R}_{\phi,k} \Gamma_k^T, \mathbf{R}_{\phi,k}^p = \Gamma_k \mathbf{R}_{\phi,k} \Gamma_{k+1}^T$ $\mathbf{U}_k^* = [(\mathbf{H}_k^*)^T (\mathbf{R}_{\phi,k}^*)^{-1} \mathbf{H}_k^*]^{-1} (\mathbf{H}_k^*)^T (\mathbf{R}_{\phi,k}^*)^{-1}$ $\bar{\mathbf{X}}_{k+1} = \hat{\mathbf{X}}_k + \mathbf{U}_{k+1}^* \Omega_{k+1}^*$ $\bar{\mathbf{P}}_{k+1} = \mathbf{U}_{k+1}^* \begin{bmatrix} \mathbf{H}_k^p \hat{\mathbf{P}}_k (\mathbf{H}_k^p)^T + \mathbf{R}_{\phi,k}^* + \mathbf{R}_{\phi,k+1}^* \\ -\mathbf{H}_k^p (I - \mathbf{K}_k^* \mathbf{H}_k^*) \mathbf{U}_k^* \mathbf{R}_{\phi,k}^p \\ -(\mathbf{U}_k^* \mathbf{R}_{\phi,k}^p)^T (I - \mathbf{K}_k^* \mathbf{H}_k^*)^T (\mathbf{H}_k^p)^T \end{bmatrix} (\mathbf{U}_{k+1}^*)^T$
Measurement Update
$\mathbf{R}_{\rho,k}^* = \Gamma_k \mathbf{R}_{\rho,k} \Gamma_k^T$ $\mathbf{K}_k^* = (\bar{\mathbf{P}}_k - \mathbf{U}_k^* \mathbf{R}_{\phi,k}^* (\mathbf{U}_k^*)^T) (\mathbf{H}_k^*)^T [\mathbf{H}_k^* \bar{\mathbf{P}}_k (\mathbf{H}_k^*)^T + \mathbf{R}_{\rho,k}^*]^{-1}$ $\mathbf{Z}_k^* = \Gamma_k \mathbf{Z}_k$ $\hat{\mathbf{X}}_k = \bar{\mathbf{X}}_k - \mathbf{K}_k^* \mathbf{Z}_k^*$ $\hat{\mathbf{P}}_k = (I - \mathbf{K}_k^* \mathbf{H}_k^*) \bar{\mathbf{P}}_k (I - \mathbf{K}_k^* \mathbf{H}_k^*)^T + \mathbf{K}_k^* \mathbf{R}_{\rho,k}^* (\mathbf{K}_k^*)^T$

The variables utilized in Table 1 are briefly explained as follows.

$$\mathbf{Z}_k = \begin{bmatrix} z_k^{1o} \\ z_k^{2o} \\ \vdots \\ z_k^{Jo} \end{bmatrix}, \Omega_{k+1} = \begin{bmatrix} \omega_{k+1}^{1o} \\ \omega_{k+1}^{2o} \\ \vdots \\ \omega_{k+1}^{Jo} \end{bmatrix}, \mathbf{H}_k = \begin{bmatrix} (e_k^{1o})^T \\ (e_k^{2o})^T \\ \vdots \\ (e_k^{Jo})^T \end{bmatrix}$$

$$z_k^{jo} = (e_k^{jo})^T \bar{X}_k - \tilde{\rho}_k^{jo}$$

$$\omega_k^{jo} = (e_k^{jo})^T \hat{X}_k - (e_{k+1}^{jo})^T \hat{X}_k (\tilde{\phi}_{k+1}^{jo} - \tilde{\phi}_k^{jo})$$

\bar{X}_k : *a priori* position estimate

\hat{X}_k : *a posteriori* position estimate

\bar{P}_k : *a priori* error covariance matrix

\hat{P}_k : *a posteriori* error covariance matrix

$R_{\rho,k}, R_{\phi,k}$: DD code and phase measurement error covariance matrix

Γ_k : channel selection matrix

$\tilde{\rho}_k^{jo}, \tilde{\phi}_k^{jo}$: DD code and phase measurement

$(e_k^{jo})^T = (e_k^j - e_k^o)^T$: difference of LOS vectors

The channel selection matrix Γ_k consists of '0's and '1's to reduce the column-vector dimension from the number of total measurements to the number of valid measurements. The channel selection matrix is also useful to consider abrupt satellite inclusions and outages.

COMPENSATION OF RECEIVER CLOCK BIAS

As widely known, receiver clock bias characteristics are diverse due to different receiver design characteristics with respect to low-cost crystal oscillators. To prevent the clock bias becoming too large, various clock steering mechanisms are utilized. The low-cost L1-only receiver considered in this study depicts its clock bias characteristics in two ways. One is the time offset included in the observation time and the other is the clock jump added only to the code measurements. If the time offset value exceeds a threshold value, the corresponding clock steering value is added to the code

measurement resulting in a clock jump.

Figure 1 show that the time offset and jump of code measurement caused by clock jump.

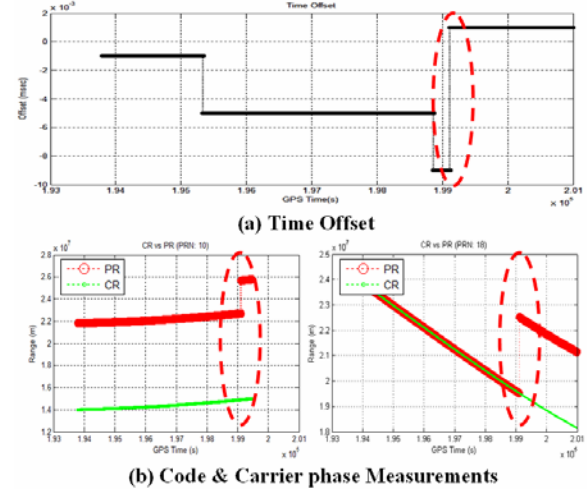


Figure 1. Time Offset and Clock Jump

The clock steering mechanism of the low-cost receiver causes the time-alignment problem in relative positioning. To solve this problem, a simple compensation algorithm is utilized as follows when there is a time offset but there is no clock jump.

- Corrected $\tilde{\rho}_k^j = \tilde{\rho}_k^j - T_{offset,k} * C$
- $\tilde{\phi}_k^j = \tilde{\phi}_k^j - T_{offset,k} * C$
- $\tilde{d}_k^j = \tilde{d}_k^j - (T_{offset,k} - T_{offset,k-1}) * C$
 $+ (T_{offset,k} - T_{offset,k-1}) * \tilde{d}_k^j$

where

$\tilde{\rho}_k^j$: code measurement

$\tilde{\phi}_k^j$: carrier phase measurement

\tilde{d}_k^j : doppler measurement

C : speed of light

$T_{offset,k}$: Time offset, k - th epoch

When there is a clock jump, an integer multiple of milliseconds is imposed on the receiver clock

bias and on the code measurements. Consequently, the clock jump can be detected following case:

$$(\tilde{\rho}_{k+1}^j - \tilde{\rho}_k^j) - (\tilde{\phi}_{k+1}^j - \tilde{\phi}_k^j) > 0.001 * C$$

The integer multiple of milliseconds can be estimated as follows:

$$N = \text{round} \left\{ \frac{0.001}{m} \sum_{i=1}^m [(\tilde{\rho}_{k+1}^i - \tilde{\rho}_k^i) - (\tilde{\phi}_{k+1}^i - \tilde{\phi}_k^i)] \right\}$$

where

N : integer multiple of milliseconds

m : number of valid satellites

Based on the estimate of N , only the carrier phase measurements are corrected by the following equation.

- Corrected $\tilde{\phi}_k^j = \tilde{\phi}_k^j - (T_{\text{offset},k} - N) * C$

By the correction procedure described so far, the corrected code and carrier phase measurements appear as the bottom plots of Figure 2 for the satellites of PRN 10 and PRN 18. The upper plot of Figure 2 corresponds to the clock bias estimate.

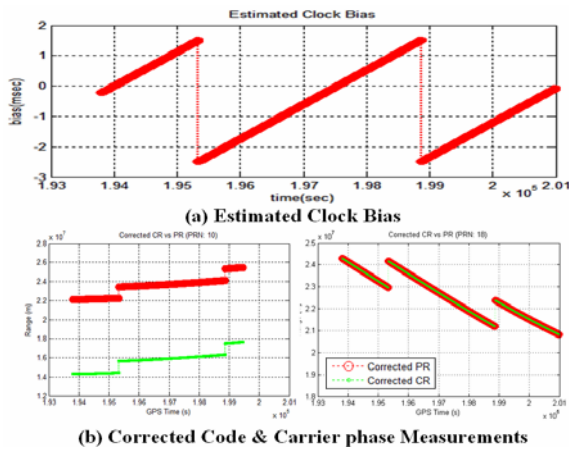


Figure 2. Estimated Clock Bias & Corrected Measurements

EXPERIMENT

To verify the performance of the proposed L1 RTK system, an experiment was performed. The experiment configuration is illustrated in Figure 3.

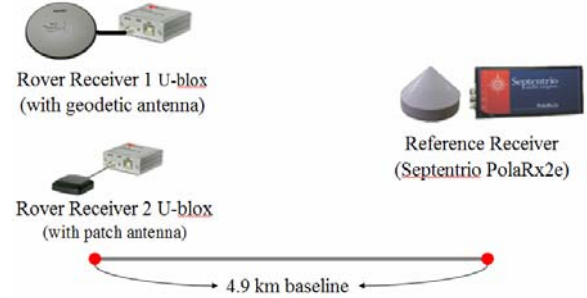


Figure 3. Configuration of Experiments

In the experiment, a dual-frequency Septentrio PolaRx2e receiver with a choke ring antenna was utilized as the reference receiver and two single-frequency U-blox AEK-4T receivers were utilized as the rover receiver. Among the two single-frequency receivers, Rover 1 was equipped with the NovAtel GPS-702-GG (geodetic grade: L1/L2) antenna and Rover 2 was equipped with the ANN-MS (consumer grade: L1 only) antenna. The baseline length between the reference and rover was 4.9km.

For data processing, the standard deviation values for the code and carrier noise terms were set as 3.0m and 0.01m, respectively. The receiver output rate was set as 1Hz and the cut-off angle for the satellite elevation angle was set as 10 degrees since the signal quality was poor at the elevation angle below 10 degrees.

Though the rover was set stationary, all the data were processed in the kinematic mode. To generate float solutions, the DD PD Hatch filter was utilized. For the integer ambiguity resolution, an ambiguity candidate was

established based on the float solution. Each integer ambiguity candidate was validated by a residual-test and a ratio-test at each epoch. If the validation results had been the same during 10 epochs, the integer ambiguity candidate was regarded as reliable.

Figure 4 shows the error distance profiles generated by L1 integer solution of Rover 1(Top) and Rover 2(Bottom). The first integer solution is fixed within approximately 500th epochs by both rover receivers. By Table 3, Table 4, and Figure 6, it can be seen that the integer solutions provides good accuracy within a few millimeter. It is anticipated that the time to first integer fix can be reduced if the sampling rate is increased from 1 Hz to 10 Hz, which is left as the topic for future study.

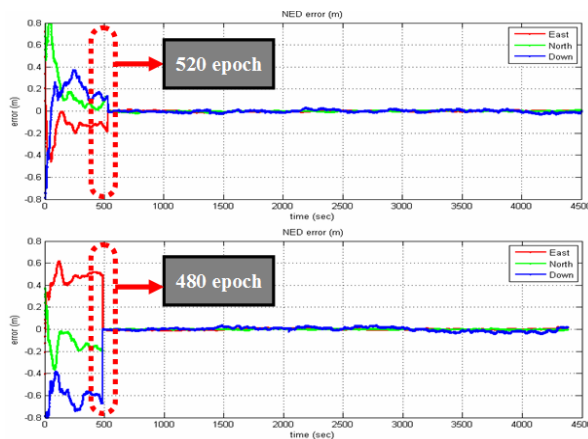


Figure 4. NED Errors of Integer Solution
(Top: geodetic antenna, Bottom: consumer antenna)

Table 2 Position Error Components (mm): Rover 1

	East error	North error	Down error
Mean	-1.3	0.3	-3.4
Std. Dev.	4.6	5.3	11.6

Table 3 Position Error Components (mm): Rover 2

	East error	North error	Down error
Mean	0.18	-0.02	-0.18
Std. Dev.	3.2	5.7	16.0

CONCLUSION AND FUTURE WORK

In this study, L1 RTK system based on DD PD Hatch filter for low cost single frequency receiver is designed and implemented. To evaluate the performance of L1 RTK system, 4.9 km static baseline experiments was performed. The experiment result shows that correct integer solutions can be obtained within approximately 500 epochs by the proposed low-cost L1 RTK system.

ACKNOWLEDGEMENTS

This research was supported by a grant from Transportation System Innovation Program (TSIP) funded by Ministry of Land, Transport and Maritime Affairs of Korean government.

REFERENCES

- [1] R.R. Hatch, "The synergism of GPS code and carrier measurements", *Proceedings of the Third International Geodetic Symposium on Satellite Doppler Positioning*, New Mexico, II, pp. 1213-1232, 1982
- [2] H.K. Lee and C. Rizos, "Position-Domain Hatch Filter for Kinematic Differential GPS/GNSS", *IEEE Transactions on Aerospace and Electronic Systems*, Vol. 44, No. 1, pp. 30-40, 2008
- [3] H.S. Kim, H.K. Lee, "Position-Domain DD Hatch Filter to Maintain Float Solution Accuracy in RTK," *Proceedings of International Symposium on GPS/GNSS 2008*, 11-14 Nov., Tokyo, 2008
- [4] D. Odijk, J. Traugott, G. Sachs, O. Montenbruck, and C. Tiberius, "Two

Precision GPS Approaches Applied to Kinematic Raw Measurements of Miniaturized L1 Receivers", *Proceedings of ION GNSS 2007*, pp. 827-838, Texas, Sept. 25-28, 2007